IBP2070_17

DUCTILE FRACTURE RESISTANCE MEASUREMENTS IN A NICKEL-CHROMIUM GIRTH WELD OF A CLAD LINE PIPE

C. Ruggieri[1], D. F. B. Sarzosa [2], V. S. Barbosa[3], E. Hippert Jr.[4]

Abstract

This work presents an exploratory investigation of the ductile tearing properties for the girth weld of a typical C-Mn pipe internally clad with a nickel-chromium corrosion resistant alloy (CRA) using experimentally measured crack growth resistance curves (CTOD – Δa curves) using the double-clip gage DCG) method. Testing of the pipeline girth weld employed side-grooved, clamped SE(T) specimens with a weld centerline notch to determine the crack growth resistance curves based upon the unloading compliance (UC) method using a single specimen technique and load-displacement records. These results are further compared with crack growth resistance data derived from a digital image correlation (DIC) method to measure the CTOD directly from the deformed crack flank for the extending crack. This exploratory experimental characterization provides additional toughness data which serve to evaluate the effectiveness of current procedures in determining experimentally measured *R*-curves for pipeline girth welds.

1. Introduction

The increasing demand for energy and natural resources has spurred a flurry of exploration and production of oil and natural gas in more hostile environments, including very deep water offshore hydrocarbon reservoirs. One of the key challenges facing the oil and gas industry is the assurance of more reliable and fail-safe operations of the infrastructure for production and transportation. Currently, structural integrity of submarine risers and flowlines conducting corrosive and aggressive hydrocarbons represents a key factor in operational safety of subsea pipelines. Advances in existing technologies favor the use of C-Mn steel pipelines either clad or mechanically lined with corrosion resistant alloys (CRA), such as UNS N06625 Alloy 625 (ASTM International B444, 2016a), for the transport of corrosive fluids. Accurate measurements of fracture resistance properties, including crack growth resistance curves of the girth weld material, become essential in defect assessment procedures of the weldment region and the heat affected zone, where undetected crack-like defects (such as lack of penetration, deep undercuts, root cracks, etc.) may further extend due to the high tension stresses and strains. However, while cost effective, fracture assessments of girth welds in lined pipes become more complex due to the dissimilar nature of these materials.

Current standardization efforts now underway (see the review article of Ruggieri (2017)) advocate the use of single edge notch tension specimens (often termed SE(T) or SENT crack configurations) to measure experimental *R*-curves more applicable to high pressure piping systems, including girth welds of marine steel risers. The primary motivation to use SE(T) fracture specimens in defect assessment procedures for this category of structural components is the strong similarity in crack-tip stress and strain fields which drive the fracture process for both crack configurations (Sarzosa and Ruggieri, 2014). Recent applications of SE(T) fracture specimens to characterize crack growth resistance properties in pipeline steels have been effective in providing larger flaw tolerances and, at the same time, reducing the otherwise excessive conservatism which arises when measuring the material fracture toughness based on high constraint, deeply-cracked, single edge notch bend (SE(B)) or compact tension (C(T)) specimens. However, while now utilized effectively in fracture testing of pipeline girth welds with limited overmatch, strong mismatch between the weld metal

[1] Professor - Faculty of Engineering, UNIVERSITY OF SÃO PAULO
[2] Assistant Professor - Faculty of Engineering, UNIVERSITY OF SÃO PAULO
[3] Ph.D. Student, Faculty of Engineering, UNIVERSITY OF SÃO PAULO
[4] Ph.D., Senior Researcher, CENPES - PETROBRAS

and base plate strength potentially affects the macroscopic mechanical behavior of the specimen in terms of its load-displacement response with a potentially strong impact on the crack growth resistance curve. Moreover, with the increased use of higher strength pipeline steels, unintended weld strength undermatching emerges as a likely possibility which thus raises strong concerns in integrity assessments of field girth welds produced in lined pipes having circumferential flaws.

Much recent research has focused on the development of standardized procedures for crack growth resistance testing using SE(T) fracture specimens (Ruggieri, 2017). Essentially all these efforts adopt primarily the unloading compliance method based upon testing of a single specimen. Implementation of the method follows conventional procedures to determine the instantaneous value of the specimen compliance at partial unloading during the measurement of the load vs. displacement curve thereby enabling accurate estimations of the *J*-integral (or, equivalently, the crack tip openibg displacement, CTOD or δ) and, crack extension, Δa, at several locations on the load-displacement records from which the $J-R$ and $\delta-R$ can be developed. While the methodology simply broadens the current framework for fracture testing of three-point bend and compact tension specimens, such as ASTM E1820 (ASTM International, 2016b), there is not much consensus on specific requirements to obtain the *J*-integral and CTOD parameters, as well as the amount of crack extension, including the estimation procedure for toughness values and compliance equations. Since the evaluation of all fracture toughness quantities represents a key step in accurate laboratory measurements of fracture resistance curves, differences in *J* and CTOD estimation equations or different compliance equations affect the experimentally measured crack growth resistance behavior thereby complicating the definition of meaningful toughness data. This picture is further complicated by the potential effect of the clad layer (which is an integral part of the SE(T) specimen extracted from girth weld clad pipes) on the mechanical response of the fracture specimen thereby affecting the amount of crack extension with increased macroscopic loading, as characterized by *J* or CTOD.

This work presents an exploratory investigation of the ductile tearing properties for the girth weld of a typical C-Mn pipe internally clad with a nickel-chromium corrosion resistant alloy (CRA) using experimentally measured crack growth resistance curves in terms of ($\mathrm{CTOD}-\Delta a$ curves). Here, the material of the external pipe is a typical API 5L Grade X65 pipeline steel with a high yield stress of 620 MPa and relatively low hardening properties whereas the inner clad layer is made of ASTM UNS N06625 Alloy 625 with yield stress of 462 MPa and high hardening. The high mechanical strength and superior resistance to a wide range of corrosive environments of unusual severity for this material derive from the combination of the nickel-chromium matrix with other microalloying elements such as molybdenum and niobium. Testing of the pipeline girth weld employed side-grooved, clamped SE(T) specimens with a weld centerline notch to determine the crack growth resistance curves based upon the unloading compliance (UC) method using a single specimen technique and load-displacement records. The crack growth resistance curves are defined in terms of $\delta-\Delta a$ data for which the CTOD is determined on the basis of J-CTOD relationships and the double clip gage (DCG) technique. These results are further compared with crack growth resistance data derived from a digital image correlation (DIC) method to measure the CTOD directly from the deformed crack flank for the extending crack. This exploratory experimental characterization provides additional toughness data which serve to evaluate the effectiveness of current procedures in determining experimentally measured *R*-curves for pipeline girth welds.

2. Overview of CTOD Resistance Test Procedure

2.1. CTOD Evaluation Procedure Based on the Double-Clip Grage Method

To provide a simpler extension of the plastic hinge concept (Anderson, 2005) applicable to broader crack configurations, a double clip-gage arrangement is often used as a simple and yet effective method to estimate the CTOD from adequate measurements of crack opening displacements (COD) at two different points. Figure 1(a) schematically illustrates the essential features of the procedure in which a pair of knife edges is attached on each side of the notch close to the notch mouth to allow the use of two clip-gages to measure the displacement at these knife edge positions - such double clip-gage (DCG) fixture is currently recommended by recent test procedures to evaluate resistance curves using SE(T) specimens, including BS 8571 (British Standards Institution, 2014) – see also Ruggieri (2017). With the method illustrated in Fig. 1(a), a simple geometrical approach then enables defining the CTOD (δ) in terms of the two measured COD-values. Here, the double clip-gage arrangement shown in Fig. 1(a) deserves attention since the DCG mounting fixture is typically installed at a distance x_0 from the notch flank as shown in Fig. 1(a); only when $x_0=0$ can the DCG fixture be considered aligned with the specimen machined notch and the fatigue precrack. This practice results in an *apparent* offset of the crack flank thereby potentially increasing the measured CTOD, here denoted as $\widetilde{\delta}$ in the figure. The specification of x_0 in the test protocol introduces an explicit dimension in the test procedure and opens the possibility to correct the measured $\mathrm{CTOD}-R$ curve for different values of x_0. However, this option was not examined in the present so that hereafter we refer to $\widetilde{\delta}$ as δ for simplicity.

Now, by measuring two COD-values, V_1 and V_2, at two locations on a straight line passing through the crack flank of the specimen and assuming rigid body rotation, a geometrical relationship between the CTOD (δ) and both measured COD-values is obtained in the form

$$\delta = V_1 - \frac{z_1 - a_0}{z_2 - z_1}(V_2 - V_1) \tag{1}$$

where z_1 and z_2 represent the distance of the measuring points for V_1 and V_2 from the specimen surface as depicted in Fig. 1(b). Here, we note that the crack size, a_0, entering into Eq. (1) represents the initial crack length not the current crack size measured at the extending tip as discussed by Sarzosa et al. (2015). Moreover, also observe that the CTOD is defined here as the crack opening at the position of the original crack tip such that, with crack-tip blunting, the position of the original crack tip falls slightly behind the current crack tip.

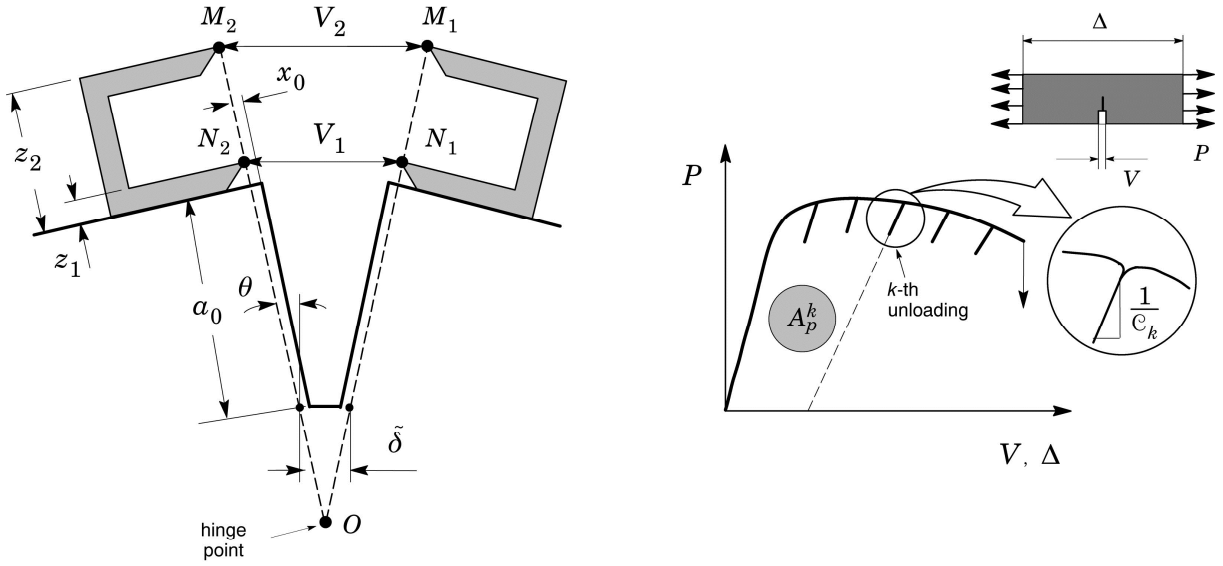

Figure 1. *(a) Double clip-gage method to estimate the CTOD using measurements of crack opening displacements (COD) at two different points. (b) Partial unloading during the evolution of load with displacement and definition of the plastic area under the load-displacement curve.*

2.2. CTOD Evaluation Procedure Based on the *J*-Integral

Since a $J-\text{CTOD}$ relationship holds true for stationary and growing cracks under certain conditions (Anderson, 2005), the crack tip opening displacement (CTOD) can be derived directly from experimentally measured records of load vs. crack mouth opening displacement (CMOD). The methodology essentially determines the CTOD value from first evaluating the plastic component of *J* using the plastic work defined by the area under the load vs. CMOD curve and then converting it into the corresponding value of plastic CTOD. The approach has the potential to simplify evaluation of CTOD values while, at the same time, relying on a rigorous energy release rate definition of *J* for a cracked body yielding the expression (Sarzosa et al., 2015)

$$\delta = \frac{J}{m\sigma_f} \tag{2}$$

in which m represents a proportionality coefficient strongly dependent on the material strain hardening but weakly sensitive to crack size as characterized by the a/W-ratio. In the above, σ_f defines the flow stress given by $\sigma_f = (\sigma_{ys} + \sigma_{uts})/2$ in which σ_{ys} is the yield stress and σ_{uts} denotes the tensile strength.

Evaluation of the *J*-integral with crack extension follows from an incremental procedure based on CMOD data (Cravero and Ruggieri, 2007) which updates *J* at each partial unloading point, denoted *k*, during the measurement of the load vs. displacement curve as

$$J^k = \left(\frac{K_I^2}{E'}\right)_k + \left[J_p^{k-1} + \frac{\eta_{J-CMOD}^{k-1}}{b_{k-1}B_N}\left(A_p^k - A_p^{k-1}\right)\right]\left[1 - \frac{\gamma_{LLD}^{k-1}}{b_{k-1}}\left(a_k - a_{k-1}\right)\right] \tag{3}$$

in which factor γ_{LLD} is evaluated from

$$\gamma_{LLD} = \left[-1 + \eta_{J-LLD}^{k-1} - \left(\frac{b_{k-1}}{W\eta_{J-LLD}^{k-1}}\frac{d\eta_{J-LLD}^{k-1}}{d(a/W)}\right)\right] \tag{4}$$

In the above, K_I is the elastic stress intensity factor for the cracked configuration, A_p is the plastic area under the load-displacement curve, B_N is the net specimen thickness at the side groove roots ($B_N = B$ if the specimen has no side grooves where *B* is the specimen gross thickness), *b* is the uncracked ligament ($b = W - a$, where *W* is the width of the cracked configuration and *a* is the crack length). In writing Eq. (3), plane-strain conditions are adopted such that $E' = E/(1-\nu^2)$ where E and υ are the (longitudinal) elastic modulus and Poisson's ratio, respectively. Factor η_J appearing in Eqs. (3) and (4) represents a nondimensional parameter which relates the plastic contribution to the strain energy for the cracked body and *J*. Figure 1(b) illustrates the essential features of the estimation procedure for the plastic component, J_p. Here, we note that A_p (and consequently η_J) can be defined in terms of load-load line displacement (LLD or Δ) data or load-crack mouth opening displacement (CMOD or *V*) data. For definiteness, these quantities are denoted η_{J-LLD} and η_{J-CMOD}.

Based on full 3-D finite element analysis of the weld centerline notched SE(T) specimen, including the clad layer, Sarzosa et al. (2017) arrived at a functional dependence of parameter *m* with crack size, a/W, in the form

$$m = 1.932 - 1.845(a/W) + 1.654(a/W)^2 \tag{5}$$

which is valid in the range $0.1 \le a/W \le 0.7$ and specifically applicable to the tested fracture specimen. Plane-strain *m*-values describing the $J-\mathrm{CTOD}$ relationship for other material properties and homogeneous specimens are also given by Sarzosa et al. (2014).

2.3. Compliance-Based Crack Extension Estimation

The slope of the load-displacement curve illustrated in Fig. 1(b) during the k-th unloading defines the current specimen compliance, denoted C_k, which depends on specimen geometry and crack length. For the clamped SE(T) configuration analyzed here, the specimen compliance based on CMOD is defined in terms of a normalized quantity expressed as

$$\mu_{CMOD} = \left[1 + \sqrt{E'B_eC_{CMOD}}\right]^{-1} \tag{6}$$

where E is the longitudinal elastic modulus, $C_{CMOD} = V/P$ denotes the specimen compliance defined in terms of crack mouth opening displacement**,** in which V is the CMOD and P represents the applied load, and the effective thickness is defined by

$$B_e = B - \frac{(B - B_N)^2}{B} \tag{7}$$

By performing a series of full 3-D finite element analysis of the weld centerline notched SE(T) specimen, including the clad layer, Sarzosa et al. (2017) showed that relationship between a/W and μ for the tested fracture specimen is described by

$$a/W = 1.6485 - 9.1005\mu + 33.025\mu^2 - 78.467\mu^3 + 97.344\mu^4 - 47.227\mu^5 \quad (8)$$

where it is understood that a 5-*th* order polynomial fitting is employed and is valid in the range $0.1 \le a/W \le 0.7$. Equation (8) defines a key step in the evaluation procedure of the crack growth resistance curve. By measuring the instantaneous compliance during unloading of the specimen (see Fig. 1(b)), the current crack length follows directly from solving the above expression for μ.

3. Experimental Details

3.1. Material Description and Welding Procedure

The material utilized in this study was a girth weld of a typical API 5L Grade X65 pipe internally clad with a nickel-chromium corrosion resistant alloy (CRA) made of UNS N06625 Alloy 625 (ASTM International B444, 2016). The tested weld joint was made from an 8-inch pipe (203 mm outer diameter) having overall thickness, $t_w = 19$ mm, which includes a clad layer thickness, $t_c = 3$ mm. Girth welding of the pipe was performed using 100% CO_2 gas-shielded FCAW process in the 1G (horizontal) position with a single V-groove configuration in which the root pass was made by TIG welding in the 2G (vertical) position. The main weld parameters used for preparation of the test weld using the FCAW process are: *i*) welding current 200 ~ 250 A; *ii*) welding voltage 27 ~ 29 V; *iii*) average wire feed speed of 11 ~ 12 m/min. A nickel-chromium filler metal matching the UNS N06625 Alloy 625 was employed to produce the girth weld so that the clad internal layer and the weld metal have very similar mechanical properties.

Table 1 provides the mechanical properties of the base plate material and the weld metal at room temperature (20°C) in which the measured values are based on standard tensile testing using subsize specimens with 6 mm diameter. The material of the external pipe has a high yield stress, σ_{ys}, of 620 MPa and relatively low hardening properties whereas the inner clad layer has yield stress of 462 MPa and high hardening. Here, we note that the measured yield stress for the external pipe is slightly higher than the maximum value of 600 MPa specified by API 5L PSL-2 (American Petroleum Institute, 2007a) for grade X65 steel - observe, however, that the yield stress to tensile strength ratio is $\sigma_{ys}/\sigma_{uts} = 0.89$, which is below the maximum specified value of 0.93 for this steel. Based on Annex F of API 579 (American Petroleum Institute, 2007b), the Ramberg-Osgood strain hardening exponents describing the stress-strain response (Anderson, 2005) for the base plate and weld metal are estimated as $n_{BM} = 18.9$ and $n_{WM} = 9.7$. The measured tensile properties indicate that the weldment undermatches the base plate by $\approx 25\,\%$ at room temperature - also observe a relatively strong mismatch in hardening behavior as characterized by the large differences in the hardening exponents. Moreover, because of the mismatch in strain hardening behavior, it can be easily anticipated that, after some amount of plastic deformation in the range of $\approx 2\,\%$, the weld metal overmatches the base plate material.

Table 1. *Tensile properties of tested girth weld at room temperature.*

Material	σ_{ys} (MPa)	σ_{uts} (MPa)	E (MPa)	σ_{ys}/σ_{uts}	n
Base plate	620	700	200150	0.89	18.9
Weld Metal	462	627	157500	0.74	9.7

3.2. Specimen Geometries

Unloading compliance (UC) tests at room temperature were performed on weld centerline notched SE(T) specimens with fixed-grip loading extracted from the girth weld of the pipe specimen in the longitudinal direction as illustrated in Fig. 2(a) to measure tearing resistance curves in terms of $J - \Delta a$ and $\text{CTOD} - \Delta a$ data. The tested SE(T) specimens have $a/W = 0.3$ and $H/W = 10$ with thickness $B = 16$ mm, width $W = 16$ mm and clamp distance $W = 160$ mm as illustrated in Fig. 2(b). Here, a is the crack depth and W is the specimen width which is slightly smaller than the pipe thickness, t_w. Conducted as part of a collaborative program between the University of São Paulo and Petrobras, testing of these specimens focused on the evaluation of crack growth resistance data for nickel-chromium girth welds made in clad line pipes.

The specimens were pre-cracked in bending using a three-point bend apparatus very similar to a conventional three-point bend test. After fatigue pre-cracking, the specimens were side-grooved to a net thickness of ~ 85% the overall thickness (7.5% side-groove on each side) to promote uniform crack growth and tested following some general guidelines described in Ruggieri and Hippert (2015). Records of load vs. crack mouth opening displacements (CMOD) were obtained for the specimens using a clip gage mounted on knife edges attached to the specimen surface. The test program covered four specimens, one of them instrumented with a double clip gage fixture as required for CMOD measurements at two different points (refer to Fig. 1(a)) and Ruggieri and Hippert (2015) for evaluation of the CTOD using the DCG method as described later in Section 4.3.

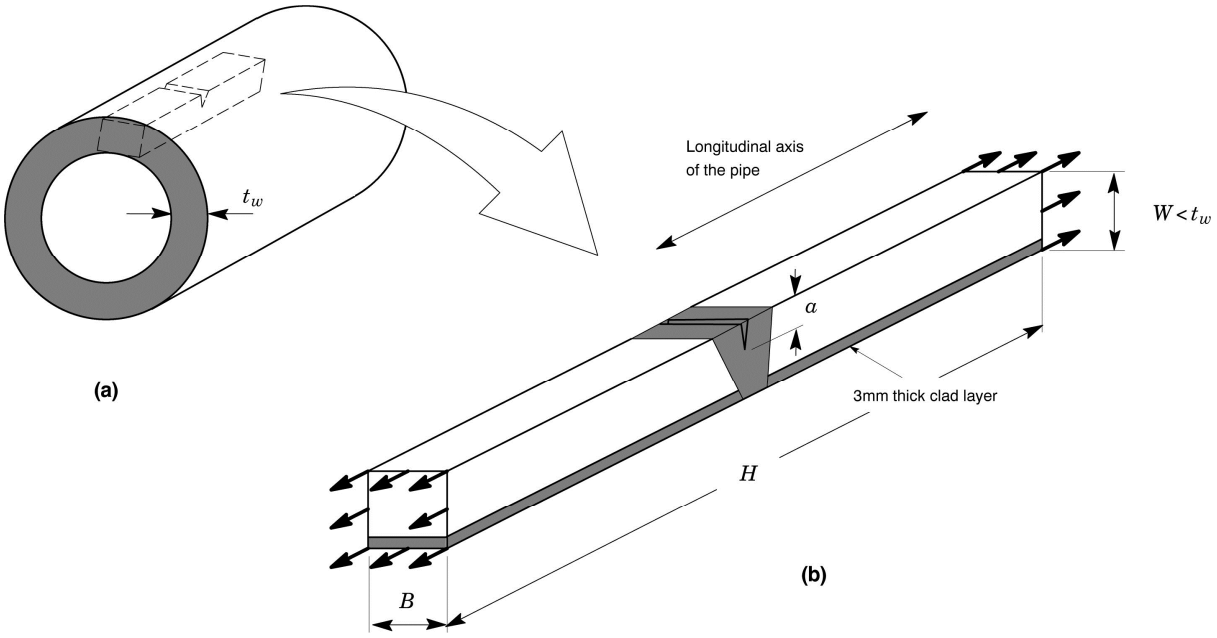

Figure 2. *Geometry of tested weld centerline notched SE(T) specimens with fixed-grip loading extracted from the girth weld of the pipe specimen in the longitudinal direction.*

4. Results and Discussion

4.1. CTOD Resistance Curves

Current defect assessment procedures applicable to piping components, including marine steel catenary risers (SCRs), often adopted by the oil and gas industry favor the use of $\text{CTOD} - R$ curves (rather than $J - \Delta a$ data) to define useful toughness values to characterize the material fracture resistance. These methodologies have evolved over the past few years to rely almost entirely on CTOD measurements derived from the double clip gage (DCG) technique outlined previously. While the merits and drawbacks of this approach remain debatable (see discussion in Sarzosa et al. (2015)), it undoubtedly simplifies the procedure to evaluate the CTOD but at an extra cost of measuring two crack opening displacements. To facilitate interpretation of the ductile tearing response for the tested nickel-chromium CRA girth weld, we also provide crack growth resistance data in terms of $\text{CTOD} - \Delta a$ curves in which the crack tip opening displacement derives from the J - CTOD relationship for the clad SE(T) specimen and from direct measurements using the DCG technique. This study also explores further direct measurements of CTOD by comparing the fracture resistance curve obtained from using a digital image correlation (DIC) method with the corresponding $\text{CTOD} - R$ curve based on the DCG technique addressed in Section 4.3.

Consider first the $\text{CTOD} - \Delta a$ curves for the tested girth weld shown in Fig. 3 in which the crack tip opening displacement is determined from the J - CTOD relationship defined by Eq. (2) with parameter m evaluated by means of Eq. (5) - these m-values thus correspond to the 3-D analysis of the weld centerline notched SE(T) specimens having a clad layer developed by Sarzosa et al. (2017). Moreover, factors η_{J-CMOD} and η_{J-LLD} needed to determine the J-integral defined by previous Eqs. (3) and (4) based on experimentally measured load vs. CMOD data are also derived

from the work of Sarzosa et al. (2017). Here, for amounts of stable crack growth of $\Delta a \approx 1\,\text{mm}$, the CTOD-value is in the range of $0.40 \sim 0.45$ mm

Evaluation of fracture resistance in terms of CTOD based on the DCG method is considered next. Here, only the load-displacement data measured from testing the specimen equipped with a double-clip gage fixture is used to generate the $\text{CTOD} - R$ curve displayed in Fig. 3. Observe that the DCG-based resistance curve is consistently higher than the $\text{CTOD} - \Delta a$ data based on *J*, particularly for larger amounts of stable crack growth, say $\Delta a \geq 1.5\,\text{mm}$. Here, differences between both methods range from $\sim 25\,\%$ for $\Delta a \approx 1.5\,\text{mm}$ to $\sim 45\,\%$ for $\Delta a \approx 3\,\text{mm}$. Further observe, however, that the CTOD resistance data based on DCG measurements increase steadily with crack growth for $\Delta a \geq 1\,\text{mm}$ such that the corresponding tearing modulus, which can be simply defined as $d\delta / da$ (Anderson, 2005), remains essentially constant. In contrast, the *J*-based CTOD resistance curves also increase with increased Δa but at a much lower rate as characterized by much smaller values of $d\delta / da$, particularly at larger amounts of ductile tearing. Allowing for some uncertainties and difficulties associated with double clip-gage measurements, these results seem generally consistent with our previous contention that, because our developed J-CTOD relationship includes effects of crack growth on *J*, the associated CTOD resistance curve should be lower than the DCG-based resistance curve. Moreover, at large deformation levels (which correspond to larger amounts of stable crack growth), much of the total work done by the applied (remote) loading is likely dissipated into background plasticity thereby reducing the plastic contribution to the strain energy for the cracked body in terms of *J*. In contrast, because the CTOD based on DCG derives from a rather simple measurement of the relative displacements of the crack profile (refer to Fig. 1(a)), it keeps increasing with increased loading. Thus, it becomes clear that the DCG-based resistance curve results in non-conservative toughness values at fixed amounts of stable crack growth thereby potentially impacting adversely ECA assessments.

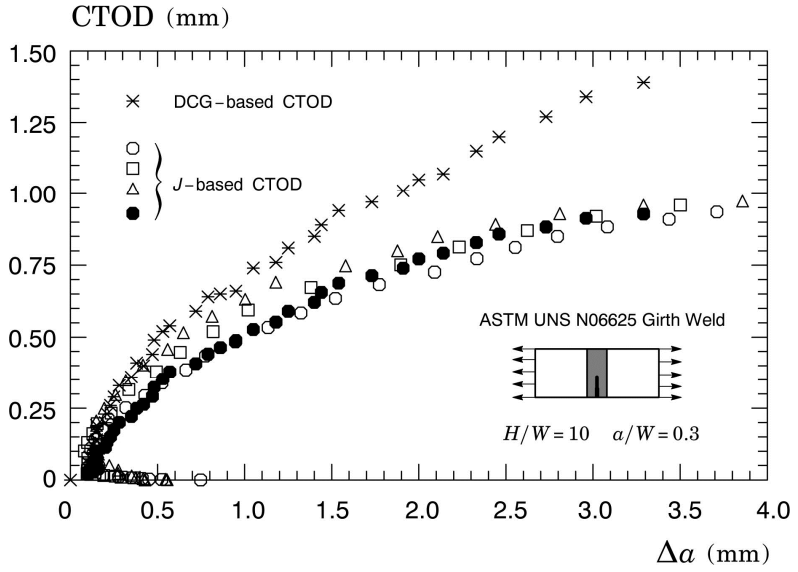

Figure 3. *CTOD-resistance curve derived from the J-CTOD relationship and the double clip-gage (DCG) method for the tested SE(T) specimen instrumented with a double clip gage fixture.*

4.2. Crack Extension Measurements

After the crack growth tests, all specimens were subjected to fatigue cycling (similar to the standard pre-crack fatigue cycling) before being broken apart to mark the new crack front and the amount of ductile tearing. A typical crack surface obtained from one of the SE(T) specimens is illustrated in Fig. 4(a), which also includes the optical crack front profile displaying the crack length measured at nine or five equally spaced points centered about the specimen centerline - the use of a 5-point average procedure to measure crack extension is addressed by Sarzosa et al. (2017). It can be seen that the specimen exhibited a somewhat non-uniform fatigue pre-crack most likely caused by microstructural heterogeneities at the crack front promoted by the welding process. Following standard methods based on the 9-point average technique, such as the procedure given by ASTM E1820 (ASTM International, 2016), the initial and final crack length measured by means of an optical method are compared with crack length estimates derived from the UC method. Figure 4(b) shows a typical fracture surface morphology to identify the primary fracture micromechanism operating

during the ductile fracture process observed by a scanning electron microscope (SEM). Here, small inclusions are observed within a dimple structure thereby characterizing well a ductile fracture mode associated with substantial plastic deformation. Similar features are also observed for the crack surface of other test specimens.

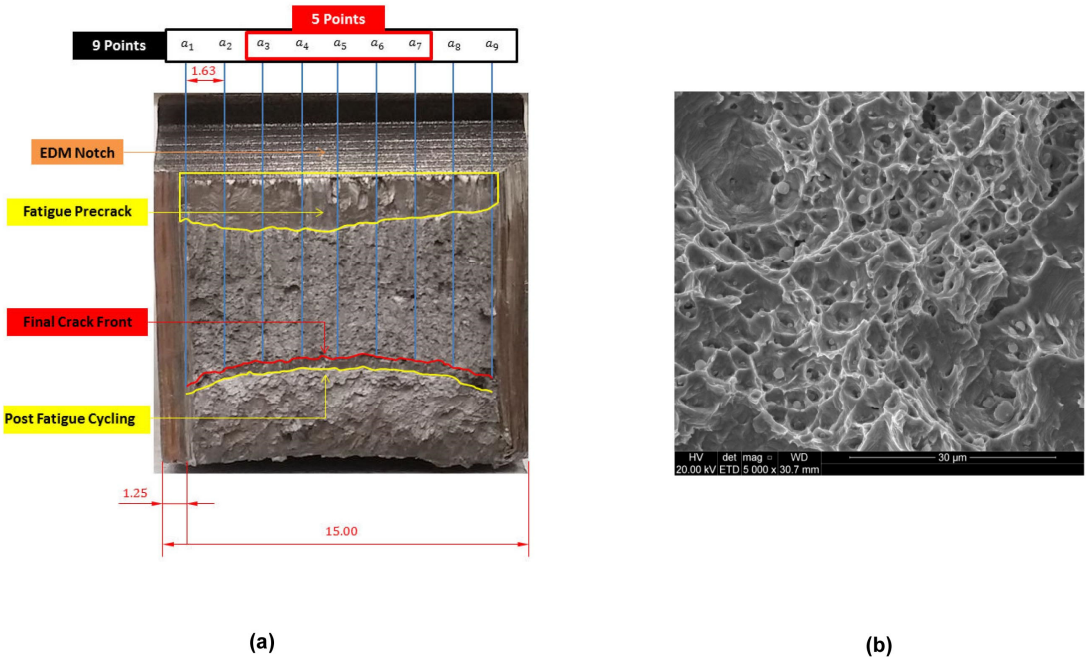

Figure 4. *(a) Typical crack surface and the optical crack size measurement profile. (b) Typical fracture surface morphology observed by a scanning electron microscope (SEM) showing small inclusions within a dimple structure.*

Table 2 provides the predicted and measured crack extension for all tested fracture specimens in which the deviation between the predicted crack growth, Δa_p, and measured crack extension, Δa_m, is defined as $\Lambda = \left|\Delta a_p - \Delta a_m\right| / \Delta a_m$. These results reveal that crack extension prediction for two of the tested specimens (CP4 and CP6) derived from the UC procedure is not in good agreement with the measured amount of ductile tearing; here, the unloading compliance method underestimates the 9-point average crack extension by 15 ~ 20% thereby plausibly producing an apparent higher *J*-resistance curve. In contrast, the predicted amount of crack extension for specimens CP5 and CP7 is in relatively good accord with the measured crack growth and shows a deviation of 5 ~ 10% between the predicted and measured data. It is worth noting that several recent procedures to measure ductile tearing properties of pipeline girth welds using SE(T) specimens (see, *e.g.*, Ruggieri and Hippert (2015)) advocate a maximum deviation, $\Lambda_{\max} = 15\,\%$, as a validity criterion. While we have not investigated further the cause of the larger deviation between the predicted and measured amount of crack growth for specimens CP4 and CP6, we argue that the relatively strong, irregular crack front profile could be a plausible reason for the relatively poor agreement between the measured and predicted amount of ductile tearing. Indeed, further examination of the fracture surface displayed in Fig. 4(a) reveals a highly non-uniform fatigue pre-crack profile, particularly near the specimen side-groove region, coupled with a relatively severe reverse tunneling of the final crack front.

4.3. Digital Image Correlation Measurements of CTOD

Concurrent with measurements of the CTOD for the growing crack based on the double clip-gage technique described in Section 4.1, an improved optical measurement method was also utilized to measure the CTOD with increased amounts of ductile tearing for the tested specimens. Using a digital image correlation (DIC) method to determine the relative displacement fields for different digital images of the cracked specimen with increased deformation, the deformed crack flank and, thus, the CTOD can be evaluated in straightforward manner. By recording a series of images during the test, each one divided into a grid of subsets, the DIC displacement measurements follow from correlating the displacement fields for the subsets at different deformation states thereby estimating the displacement field from one image to the following one. In the present study, an 8-megapixel, monochromatic digital

camera was used for image acquisition. Correlated Solutions VIC-2D V6.0 software was used for all data acquisition, calibration and DIC data analysis.

CTOD-values during crack growth in the SE(T) specimen are evaluated from DIC measurements using the scheme adopted by Sarzosa et al (2017), which is based on placing the measurement points on the fatigue pre-crack flank slightly behind the extending crack flank. As already outlined in previous Section 2.1, since the DCG mounting fixture is typically installed at a distance x_0 from the notch flank indicated in Fig 1(a), placing the measurement points on the deformed flanks of the fatigue pre-crack presumably provides a better characterization of the local displacement fields than the DCG method (which may result in an apparent increase of the measured CTOD value). Consequently, we can anticipate a more accurate evaluation of the CTOD for the growing crack even though the CTOD (δ) is still defined at the original crack tip position - see Fig. 1(a) in which the CTOD is defined as the crack opening at the crack length a_0. Here, by measuring two COD-values, V_1 and V_2, at two locations on the fatigue pre-crack flank, the CTOD is determined in straightforward manner by simple triangulation.

Figure 5 displays the CTOD resistance curve based on DIC measurements of crack opening displacements for the fatigue pre-crack flank. To facilitate comparisons, the DIC measurements are performed on the same tested SE(T) specimen instrumented with a double clip gage fixture. The previous results for the $\text{CTOD} - R$ curves are also included to aid in assessing the relative change in fracture resistance data. This figure shows clearly the effect of different measurement points (upon which the triangulation defining parameter δ is based) on the CTOD-value. The DIC-based CTOD resistance curve is now closer to the fracture resistance curves obtained by using the J-CTOD relationship. In particular, the DIC-based data agrees well with the $\text{CTOD} - R$ curves derived from J for amounts of ductile tearing in the range $\Delta a \leq 2$ mm. Observe, however, that the CTOD resistance data based on DIC measurements also increase steadily with crack growth for $\Delta a > 2$ mm such that the corresponding tearing modulus remains essentially constant - this behavior is similar to the DCG-based $\text{CTOD} - R$ curve shown in previous section.

Table 2. Predicted and measured crack extension for all tested fracture specimens using a 9-point averaging procedure.

Specimen	Measured Post Test			Compliance Estimation			Deviation
	a_0 (mm)	a_f (mm)	Δa (mm)	a_0 (mm)	a_f (mm)	Δa (mm)	Λ (%)
CP4	5.0	10.6	5.6	5.0	9.7	4.7	16.3
CP5	4.7	10.6	5.8	4.8	11.0	6.2	6.3
CP6	4.8	9.6	4.8	5.0	8.9	3.8	19.7
CP7	4.4	8.1	3.7	4.7	8.0	3.3	9.9

5. Concluding Remarks

This study presents an exploratory experimental investigation of the crack growth resistance properties for the girth weld of an API 5L Grade X65 internally clad with a nickel-chromium corrosion resistant alloy (CRA) of ASTM UNS N06625 Alloy 625. Testing of the pipeline girth welds employed side-grooved, clamped SE(T) specimens with a weld centerline notch to determine the crack growth resistance curves based upon the unloading compliance (UC) method using a single specimen technique. The experiments and fracture resistance data described in this paper show the effectiveness of the UC procedure to characterize ductile tearing properties for dissimilar girth weld materials which serve as a basis for ductile tearing assessments in ECA procedures applicable to clad pipeline girth welds and similar structural components.

A key observation emerging from our work is that the CTOD evaluation procedure based on the DCG technique shows a clear tendency to provide higher fracture resistance curves and, consequently, non-conservative fracture assessments. In contrast, DIC measurements of CTOD based on crack flank measurement points provide good agreement with the $\text{CTOD} - R$ curve evaluation procedure based on the developed J-CTOD relationship for the clad SE(T) specimen. The analyses and test results described here thus suggest that the use of $\text{CTOD} - R$ curves to measure crack growth properties for pipeline girth welds and similar structural components based on J-CTOD relationships may eliminate the potential non-conservatism that would otherwise arise when using DCG-based $\text{CTOD} - R$ curves. Clearly, more experimental and analytical studies are needed to clarify the significance of CTOD measurements for growing cracks - this issue appears central to develop a more robust and meaningful CTOD-resistance evaluation

procedure. Additional work is in progress along this line of investigation covering crack growth resistance testing based on the UC procedure of two widely different hardening steels using clamped SE(T) fracture specimens.

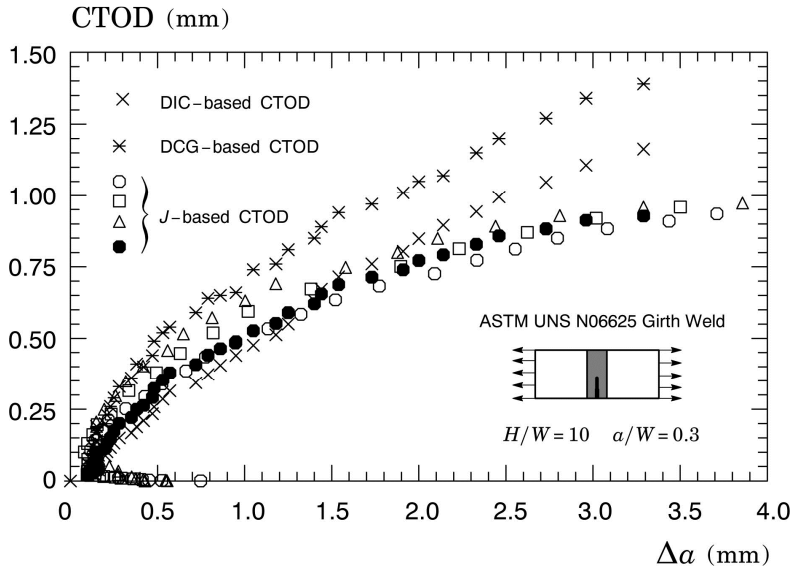

Figure 5. *CTOD-resistance curve derived from measurements of crack opening displacements for the fatigue pre-crack flank using a digital image correlation (DIC) technique.*

7. Acknowledgements

This investigation is supported by the Brazilian Council for Scientific and Technological Development (CNPq) through Grants 473975/2012-2 and 306193/2013-2. The authors acknowledge Petrobras for providing additional support for the work described here and for making available the experimental data. The authors are also indebted to Prof. C. P. Pesce (University of São Paulo) for his assistance in implementing the digital image correlation (DIC) system. Helpful discussions with Dr. Rafael G. Savioli (University of São Paulo) are also acknowledged.

8. References

AMERICAN PETROLEUM INSTITUTE, Specification for Line Pipe, *API 5L*, 2007a.

AMERICAN PETROLEUM INSTITUTE, Fitness-for-Service, *API RP-579-1/ASME FFS-1*, 2007b.

ANDERSON, T. L., Fracture Mechanics: Fundaments and Applications - 3rd Edition, CRC Press, 2005.

ASTM INTERNATIONAL, Standard Specification for Nickel-Chromium-Molybdenum-Columbium Alloys (UNS N06625 and UNS N06852) and Nickel-ChromiumMolybdenum-Silicon Alloy (UNS N06219) Pipe and Tube. *ASTM B444*, 2016a.

ASTM INTERNATIONAL, Standard Test Method for Measurement of Fracture Toughness. *ASTM E1820*, 2016b.

BRITISH STANDARDS INSTITUTION, Method of Test for Determination of Fracture Toughness in Metallic Materials Using Single Edge Notched Tension (SENT) Specimens. *BS 8571*, 2014.

CRAVERO, S., RUGGIERI, C., Further Developments in *J* Evaluation Procedure for Growing Cracks based on LLD and CMOD Data. *International Journal Fracture*, Vol. 148, pp. 387-400, 2007.

RUGGIERI C, HIPPERT E., Test Procedure for Fracture Resistance Characterization of Pipeline Steels and Pipeline Girth Welds Using Single-Edge Notched Tension (SENT) Specimens. University of São Paulo, Technical Report, 2015.

RUGGIERI, C., Low Constraint Fracture Toughness Testing using SE(T) and SE(B) Specimens. *International Journal of Pressure Vessels and Piping*, 2017 (Accepted for Publication).

SARZOSA, D. F. B., RUGGIERI, C., A Numerical Investigation of Constraint Effects in Circumferentially Cracked Pipes and Fracture Specimens Including Ductile Tearing. *International Journal of Pressure Vessels and Piping*, Vol. 120-121, pp. 1-18, 2014.

SARZOSA, D. F. B., SOUZA, R. F., RUGGIERI, C., *J*-CTOD Relations in Clamped SE(T) Fracture Specimens Including 3-D Stationary and Growth Analysis. *Engineering Fracture Mechanics*, Vol. 147, pp. 331-354, 2015.

SARZOSA, D. F. B., BARBOSA, V. S. SANTOS, C. C. P., HIPPERT, E. RUGGIERI, C., Fracture Resistance Testing of Dissimilar Nickel-Chromium Girth Welds for Clad Line Pipes. *International Journal of Fracture*, Vol. 205, pp. 169-188, 2017.